Hindawi Publishing Corporation
Advances in Materials Science and Engineering
Volume 2012, Article ID 525428, 8 pages
doi:10.1155/2012/525428

Research Article

Crystallisation Kinetics of a β-Spodumene-Based Glass Ceramic

Oscar Rubem Klegues Montedo,[1] Dachamir Hotza,[2] Antonio Pedro Novaes de Oliveira,[2] Robert Meszaros,[3] Nahum Travitzky,[3] and Peter Greil[3]

[1] *Unidade Acadêmica de Ciências, Engenharias e Tecnologias (UNACET), Universidade do Extremo Sul Catarinense (UNESC), 88806-000 Criciúma, SC, Brazil*
[2] *Group of Ceramic and Glass Materials (CERMAT), Department of Mechanical Engineering (EMC), Federal University of Santa Catarina (UFSC), 88040-900 Florianópolis, SC, Brazil*
[3] *Department of Materials Science, Institute of Glass and Ceramics, University of Erlangen-Nuremberg, 91058 Erlangen, Germany*

Correspondence should be addressed to Oscar Rubem Klegues Montedo, oscar.rkm@gmail.com

Received 25 February 2011; Revised 19 September 2011; Accepted 20 September 2011

Academic Editor: Joseph Lai

LZSA (Li_2O-ZrO_2-SiO_2-Al_2O_3) glass ceramic system has shown high potential to obtain LTCC laminate tapes at low sintering temperature (<1000°C) for several applications, such as screen-printed electronic components. Furthermore, LZSA glass ceramics offer interesting mechanical, chemical, and thermal properties, which make LZSA also a potential candidate for fabricating multilayered structures processed by Laminated Objects Manufacturing (LOM) technology. The crystallization kinetics of an LZSA glass ceramic with a composition of $16.9Li_2O \cdot 5.0ZrO_2 \cdot 65.1SiO_2 \cdot 8.6Al_2O_3$ was investigated using nonisothermal methods by differential thermal analysis and scanning electronic microscopy. Apparent activation energy for crystallization was found to be in the 274–292 $kJ \cdot mol^{-1}$ range, and an Avrami parameter n of 1 was obtained that is compared very favorably with SEM observations.

1. Introduction

A considerable effort has been spent to obtain high-performance glass ceramics for several potential applications in the medical, automotive, and telecommunication fields [1]. Low-temperature cofired ceramics (LTCCs) have created good perspectives for those applications, with special attention to the glass ceramic materials [2, 3]. LZSA glass ceramics (Li_2O-ZrO_2-SiO_2-Al_2O_3) have been studied because of their beneficial thermal, mechanical, and thermal properties [4], among other interesting features. Moreover, laminated LZSA bodies crystallized at 850°C/30 min have demonstrated to exhibit a low dielectric constant of 8.61 ± 0.84 at 1 MHz (room temperature) [5]. Furthermore, their relatively low temperatures of sintering [6] make β-spodumene-based glass ceramics (LZSA) a potential candidate for obtaining multilayered structures processed by LOM technology (Laminated Objects Manufacturing) [7]. However, the low sintering temperature is also accomplished by low crystallization temperature in this system, especially for very fine powders and low heating rates. In order to control thermal treatment for obtaining optimized properties, it is necessary to determine the kinetics parameters of crystallization for this glass ceramic system.

Isothermal crystallization kinetics of glass ceramic systems commonly refers to the following well-established Johnson-Mehl-Avrami equation [8]:

$$-\ln(1-x) = kt^n, \tag{1}$$

where x is the volume fraction crystallized at a given temperature and time t, n is the Avrami parameter related to the nucleation and crystal growth mechanisms, and k is the reaction rate constant related to the apparent activation energy for crystallization, E_c. Nonisothermal conditions have been more largely widespread in the crystallization studies

Table 1: Chemical composition of LZSA parent glass.

Oxides	Glass composition, mol%
SiO_2	65.1
Al_2O_3	8.6
Na_2O	0.6
K_2O	0.4
Li_2O	16.9
CaO	0.6
MgO	2.0
ZrO_2	5.0
BaO	0.2
ZnO	0.6

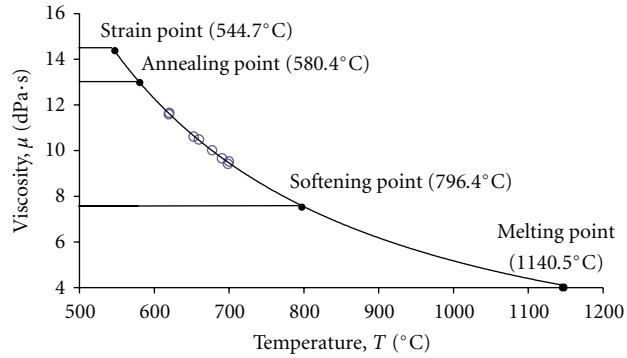

Figure 1: Viscosity of the selected glass in function to the temperature.

of amorphous materials [3, 9–15], despite the scepticism of Shaaban [16]. According to Shaaban [16], Kissinger plot and Ozawa plot cannot be directly used for crystallization of amorphous materials, because crystallization is advanced by the nucleation and crystal growth process instead of by nth order reaction. However, most of work reported in the literature used DTA or DSC to determine the kinetics parameters E_c and n. Measurements using dilatometer were also applied in some cases [17, 18].

Those methods, which assume that deflection from the baseline is proportional to the instantaneous reaction rate, require a uniform temperature of the sample independently of the heating rate. This is obtained employing small samples and low heating rates during heat treatments [9].

The aim of this work is to present the results of an investigation about the crystallization kinetics of a β-spodumene-(LiAl $[Si_2O_6]$) based LZSA glass ceramic composition by means of Nonisothermal method.

2. Material and Methods

2.1. Samples Preparation. A β-spodumene-based glass ceramic composition with interesting chemical, thermal, and electrical (dielectric constant) properties [4, 5] was selected and prepared from suitable amounts of Li_2CO_3, $ZrSiO_4$, SiO_2, and $LiAl[Si_2O_6]$ (spodumene, Colorminas Colorifício e Mineração, Criciúma, Brazil). The powders were mixed and melted at 1550 ± 3°C for 2 h in a gas furnace using a mullite crucible. The melt was poured into deionized water and the quenched frit powder was remelted at 1550 ± 2°C for 2 h in an electric furnace (Nabertherm LHT 02/17 LBR, Nabertherm, Lilienthal, Germany) using an alumina crucible to finally obtain a homogeneous viscous liquid. Chemical analysis is shown in Table 1. A small amount of the obtained melt was poured into a graphite crucible, transferred to an annealing furnace (Linn High Therm LM 421.27, Linn High Therm, Eschenfelden, Germany) and held at 570°C for 1 h to obtain small monoliths (50 mm × 5 mm × 4 mm) that were used to determine the glass transition temperature (T_g) by beam-bending test (Beam-Bending Viscosimeter, Bähr Thermoanalyse VIS 401, Hüllhorst, Germany) applying a constant heating rate of 10°C·min^{-1}. Thermal expansion was measured with a horizontal dilatometer (DIL 402C, Netzsch, Selb, Germany) at the same heating rate. From the remaining glass frit a powder fraction of 0.5–0.7 mm was prepared and subsequently dry-milled in a porcelain ball mill for 3 h. The particle size was determined by laser granulometric analysis (Cilas 1064L particle size analyzer, Orleans, France). Theoretical densities of glass powder and glass ceramic obtained at different temperatures were measured by He pycnometry (AccuPyc 1330, Micromeritics, Norcross, GA; 5 measurements). Apparent geometric densities of the compacted bodies (40 MPa, 1.4 g·cm^{-3} green density) were determined geometrically. Relative densities at several temperatures were calculated taking into account the ratio between apparent and theoretical densities of the heat-treated samples. Dielectric constant measurements were carried out according to DIN 53 482/VDE 0303 in a HP Dielectric Test Fixture (16451B, Hewlett Packard, Waldhausen, Germany) at room temperature applying a frequency of 1 MHz. The samples were discs of 20 mm × 1.2 mm heat-treated at 850°C for 10 min.

2.2. Determination of the Predominant Crystallization Mechanism. The method of Thakur and Thiagarajan [19] was used to determine the nucleating efficiency, in which the variation in onset of crystallization, ΔT_x, with particle size was monitored in a differential scanning calorimeter (DSC 404C, Netzsch, Selb, Germany; alumina crucibles, dry air). A constant heating rate of 10°C·min^{-1} was applied to determine the predominant crystallization mechanism. Moreover, a small monolith sample (5 mm × 4 mm × 4 mm) was polishing to eliminate apparent surface defects and subsequently heat-treated at 875°C for 2 h (10°C·min^{-1}).

2.3. Identification of the Crystalline Phases Formed. High-temperature X-ray diffraction (HT-XRD) patterns were recorded (Siemens D500, Siemens AG, Mannheim, Germany) from powdered samples. Monochromated Cu Kα1 radiation was applied at a voltage of 30 kV and a current of 30 mA.

2.4. Crystallisation Kinetics Investigation. The onset of crystallization T_c was determined by differential thermal analysis

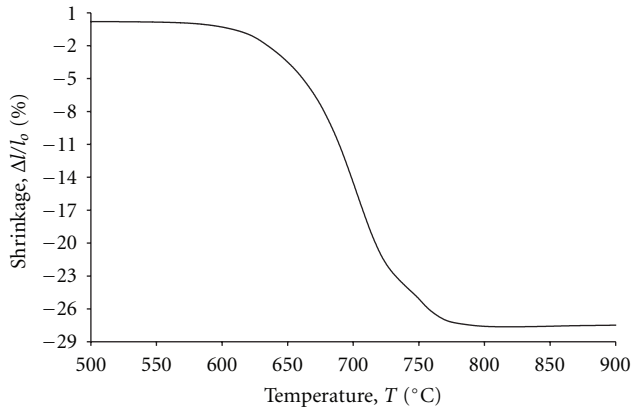

Figure 2: Linear shrinkage versus temperature of the selected glass.

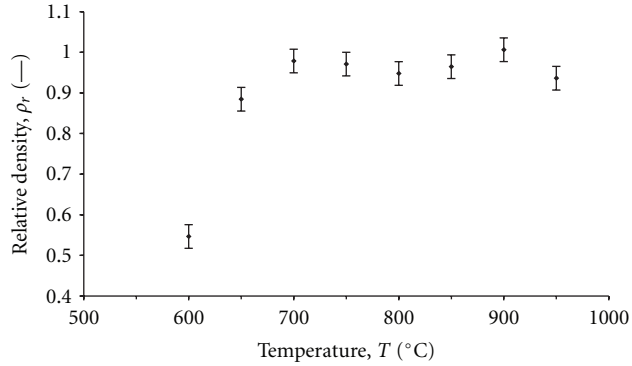

Figure 3: Relative density versus temperature of the selected glass.

Table 2: Properties of the investigated LZSA glass ceramic (sintered at 850°C for 10 min).

d_{50}, μm	2.34
ρ, g·cm^{-3}	
Parent glass	2.622 ± 0.004
Glass ceramic	2.711 ± 0.003
α, 10^6 °C^{-1}	2.38
tan δ	0.029 ± 0.011
ε_r	9.97 ± 0.84
T_g, °C	580
T_c, °C	794
$T_c - T_g$, °C	214

(DTA STA 429, Netzsch, Selb, Germany; alumina crucibles, dry air) at 5, 10, 15, and 20°C·min^{-1} heating rates.

2.5. Crystal Growth Investigation. Monoliths (50 mm × 5 mm × 4 mm) were prepared from the transparent glass samples. Some of them were cut in small pieces of 5 mm × 4 mm × 4 mm which were used for investigating the crystal growth under different heat treatment conditions in an electrically heated furnace (LM 421.27, Linn High Therm, Eschenfelden, Germany). Temperatures of 700, 750, 775, 800, 825, 850, 875, and 900°C and swelling times of 15, 30, 60, and 120 min were applied. After heat treatment, each sample was transversally cut. Morphology, crystal formation, and crystalline growth from surface towards to the centre of the monoliths were analysed by scanning electronic microscopy (SEM, Philips XL 30, Eindhoven, The Netherlands).

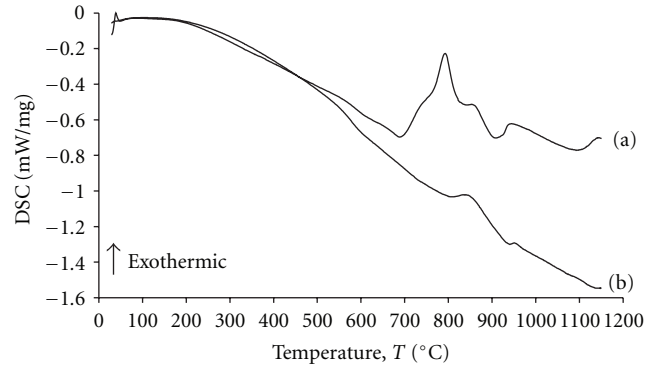

Figure 4: DSC scans at 10°C·min^{-1} heating rate for different glass powders: (a) 2.34 μm mean particle size; (b) 0.5–0.7 mm size.

2.6. Determination of the Activation Energy for Structural Relaxation. The activation energy for structural relaxation was determined for the investigated composition by means of the method of Moynihan et al. [20] Small monoliths (20 mm × 5 mm × 4 mm) were analyzed to determine the glass transition temperature (T_g) according to DIN 52324 (*Bestimmung der Transformationstemperatur*) with a horizontal dilatometer (DIL 402C, Netzsch, Selb, Germany; dry air). However, the last heating run to determine T_g was performed at 5, 10, 15, and 20°C·min^{-1} heating rates.

3. Results and Discussion

Some basic properties of the selected glass are summarized in Table 2. Taking into account this glass presents T_g of 580°C (Figure 1), determined by beam-bending test, and sintering in glasses occurs by viscous flow, densification would be expected to start around T_g. In fact, Figure 2 shows that sintering started at about 600°C and maximum shrinkage was achieved at 800–850°C. This result compares very favorably with relative density data, Figure 3. By means of optimized heat treatment (30 min at 700°C and 10 min at 850°C), a low-porosity (3.2%), low-CET (2.38 × 10^{-6}°C^{-1}), and low-dielectric constant (9.97 ± 0.84) material was obtained.

3.1. Crystallization and Particle Size. According to previous work [4], very fine powders of β-spodumene-based glass ceramics show crystallization on the surface rather than in the bulk because of very high specific surface area. Figure 4 shows DSC of two LSZA glass powders differing in size: powder *a* is of small grain size ($d_{50} \sim 2.34\,\mu$m) and exhibits a pronounced exothermic peak centered at approximately 790°C indicating intensive crystallization of β-LiAl[Si_2O_6]

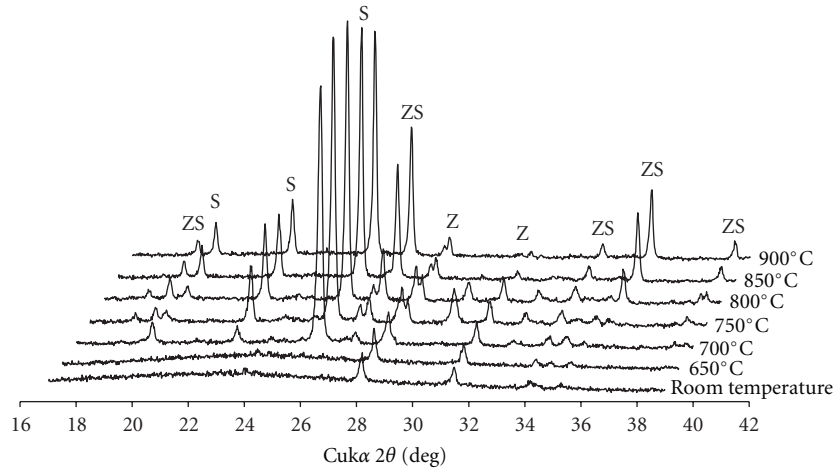

Figure 5: HT-XRD patterns recorded on a powdered sample in the specified temperatures: S: β-LiAl[Si_2O_6]-ss; ZS: $ZrSiO_4$; Z: ZrO_2.

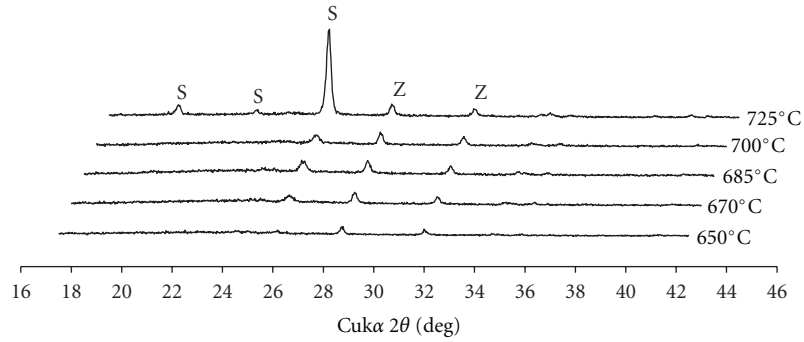

Figure 6: XRD patterns recorded of the samples after heat treatment for 10 min in the specified temperatures: S: β-LiAl[Si_2O_6]-ss; ZS: $ZrSiO_4$; Z: ZrO_2.

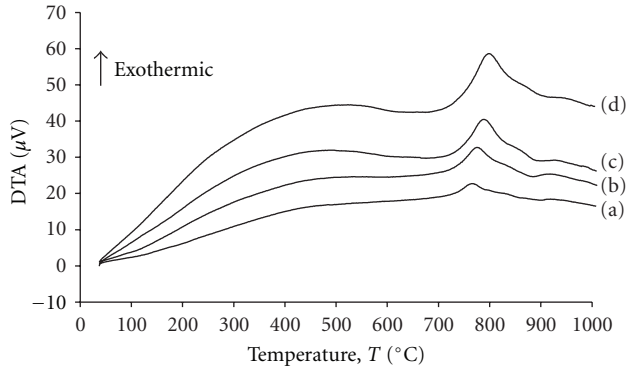

Figure 7: DTA scans at different heating rates of the selected glass: (a) 5°C·min^{-1}; (b) 10°C·min^{-1}; (c) 15°C·min^{-1}; (d) 20°C·min^{-1}.

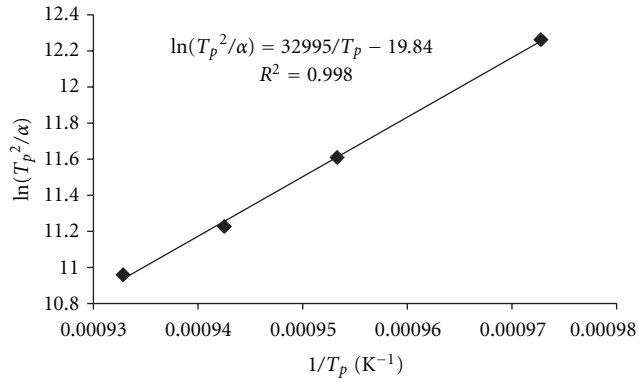

Figure 8: Apparent activation energy for crystallization plot for the selected glass based on (2) with $n = m = 1$.

during heating; powder *b* has a significantly larger particle size ($d_{50} \sim 500$–$700\,\mu$m) and a small peak at approximately 840°C. Thus, with decreasing particle size, the temperature of the exothermic peak maximum was shifted to lower temperatures. From the magnitude of the peak temperature shift with the particle size, ΔT_x, it was concluded that surface crystallization should dominate over volume crystallization when $\Delta T_x > 20$°C whereas volumetric crystallization was expected to prevail for $\Delta T_x < 10$°C [19]. Since for the LSZA glass $\Delta T_x \sim 50$°C for the two grain sizes studied surface crystallization is concluded to dominate devitrification which is in good agreement with previous work for similar glasses [4]. Thus, the results confirm a distinct particle size effect on the

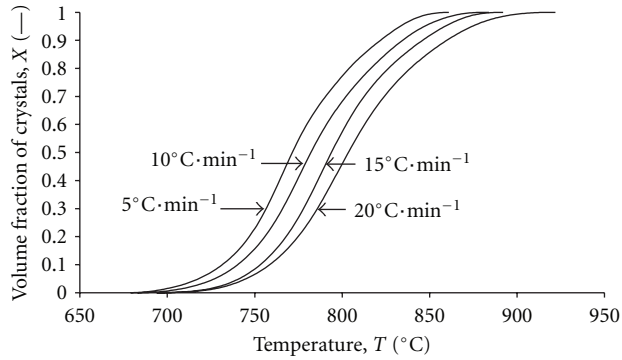

Figure 9: Measurement of the crystallization progress from normalization and integration of the DTA scans.

crystallization of β-LiAl[Si_2O_6] which for small particle sizes will be dominated mainly by surface crystallization. Hence, for larger particle size, crystallization rate will be slower and volumetric crystallization will increase at a given heating rate [14].

3.2. Crystalline Phase Composition. HT-XRD patterns recorded on a powdered sample in the temperature range of 650–950°C are shown in Figure 5. Additional powder samples were prepared and heat-treated at 650, 670, 685, 700, and 725°C for 10 min in order to obtain new XRD patterns as shown in Figure 6. At room temperature the material is essentially vitreous except for traces of zirconia (monoclinic ZrO_2, m-ZrO_2) (Figure 5). Due to the limited cooling rate and small solubility, precipitation of m-ZrO_2 may have occurred even during quenching. Crystallization of β-spodumene solid solution ($Li_{0-6}Al_{0-6}Si_{2-4}O_6$, ICCD card no. 21-503; $LiAlSi_3O_8$, ICCD card no. 15-27) was found to commence at approximately 670°C (Figure 6). A pronounced acceleration was observed at temperatures above 725°C. The peak maxima occurred at 800°C which coincides with the results of DTA measurements. Above 750°C zircon ($ZrSiO_4$, ICCD card no. 6-266) crystallized as the second major phase with maxima reached at 900°C (Figure 5).

3.3. Crystallization Kinetics. DTA and DSC have widely been used to evaluate Nonisothermal crystallization kinetics [14–16, 21–23]. Based on the variation in peak crystallization temperature (T_p) with heating rate ($\alpha = dT/dt$) the apparent activation energy for crystallization, E_c, was derived from Matusita and Sakka's [22] modification of the Kissinger [21] equation:

$$\ln\left(\frac{\alpha^n}{T_p^2}\right) = -\left(\frac{mE_c}{RT_p}\right) + C, \tag{2}$$

where n and m are numerical factors related to the crystallization mechanism [12], R is the gas constant, and C is a constant. For the case when crystallization is dominated by three-dimensional crystal growth, $n = m = 3$, and for predominantly surface crystallization, $n = m = 1$. A plot of $\ln(T_p^2/\alpha^n)$ against $1/T_p$ should give a straight line with slope (E_c/R). The value of the Avrami parameter n was evaluated from a common method developed by Augis and Bennett [23]:

$$n = \frac{2.5RT_p^2}{E_c \Delta w}, \tag{3}$$

where Δw is the full width of the DTA exothermic peak at the half maximum and E_c was calculated from (2). Avrami parameter n was found to be in the range of 1.0 and 1.2 and can be adjusted to a value of 1, confirming that the glass shows crystallization by surface mechanism. Then, one can consider $n = m = 1$ [9], taking into account that crystallization at different heating rates occurs on a fixed number of nuclei, and (3) can be reduced to the Kissinger equation [20].

Table 3: Onset temperature for each heating rate investigated.

Heating rates	T_p (°C)
5°C·min^{-1}	755
10°C·min^{-1}	776
15°C·min^{-1}	788
20°C·min^{-1}	799

Typical DTA scans of glasses subjected to different heating rates from 5°C/min to 20°C/min are shown in Figure 7, while T_p values are summarized in Table 3. The peak temperature T_p of the exothermic peak associated with crystallization of β-spodumene$_{ss}$ increased from 755°C to 799°C with increasing heating rate. However, the exothermic event related to zircon crystallization is not well defined, although it was clearly recorded in the XRD patterns.

Apparent activation energy for crystallization plot is given in Figure 8. The linearity of the curve obtained for these plots suggests that a fixed number of nuclei were achieved in the crystallization [24]. Taking $n = m = 1$ values of $E_c \sim 274$ kJ/mol and $n \sim 1.2$ were derived. Hu et al. [25] reported E_c values of 415 kJ·mol^{-1} for crystallization of β-quartz$_{ss}$ and β-spodumene crystalline phases, whilst Lee et al. [24] measured 285 kJ·mol^{-1} for crystallization of β-eucryptite (β-LiAl [SiO_4]).

The area under the exothermic peak can provide information about the evolution of the crystallization process. Considering the area under the exothermic peak (DTA scan) for each temperature that is proportional to the volumetric fraction of crystals (X), the crystallization progress by DTA scans with different heating rates was also evaluated (Figure 9). For each heating rate, the curves assumed typical sigmoidal shape. Crystallization started at approximately 700°C independently on all the heating rate but finished at higher temperatures as the heating rate was increased. The incubation time (τ), that is, the time necessary for β-spodumene$_{ss}$ crystalline phase development, increases with heating rate increasing. Thus, the improvement of densification could be achieved at 20°C·min^{-1} heating rate.

3.4. Microstructure. Figure 10 shows SEM micrographs of the microstructures observed in the parent and crystallized

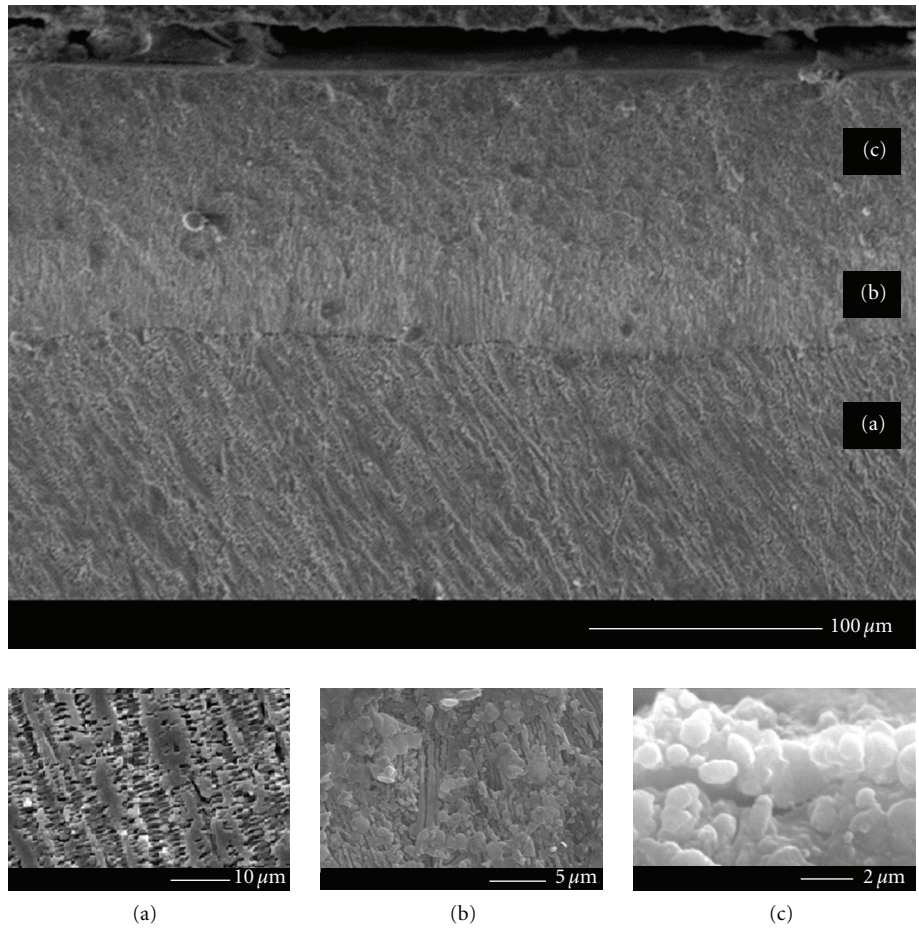

FIGURE 10: SEM image of β-spodumene-based glass ceramic monolith prepared at 875°C for 15 min: (a) parent glass; (b) first crystallization front; (c) second crystallization front.

LZSA glass ceramic. Distinct differences in morphology and distribution of crystalline precipitations are related to different stages of the crystallization process. At the beginning of the crystallization process, columnar crystals of β-spodumene$_{ss}$ with a typical grain size of $\sim 4\,\mu$m form that preferentially grow perpendicular from the surface (Figure 10(b)). This one-dimensional growth pattern is in agreement with Avrami parameter obtained ($n \sim 1.2$). With increasing crystallization time at 875°C, however, crystallites tend to form spherical particles with grain sizes of 1 μm (Figure 10(c)). According to the DTA data and XRD patterns, the second front of crystalline growing should be related to the formation of zircon in the presence of β-spodumene$_{ss}$.

3.5. Determination of the Activation Energy of Structural Relaxation. The activation energy of structural relaxation, E_{relax}, can be related to the activation energy of viscous flow. The value for E_{relax} should give an indication of the sintering ability of a glass powder system [26]. The activation energy of structural relaxation was calculated according to the relation of Moynihan et al. [20]:

$$\ln \alpha = -\frac{E_{\text{relax}}}{\text{R}T_g}. \tag{4}$$

Values of glass transition temperature, T_g, for the different heating rates were 589°C (α = 5°C/min), 600°C (10°C/min), and 607°C (15°C/min). The activation energy of structural relaxation derived from these data attained a value of $E_{\text{relax}} \sim 386$ kJ/mol which significantly is higher than the activation energy for crystallization.

Regarding the powdered glass features (composition, mean particle size, and thermal properties), processing characteristics (temperatures and heating rates), and the final properties of the obtained glass ceramic, some properties were improved such as porosity, despite the small temperature range for sintering, and CTE. However, the control of crystallization (temperature and time) can be used to create a three-layered structure with specific thickness of each layer from glass monoliths. An internal, thinner layer mostly formed by crystals of β-spodumene$_{ss}$ and an external, coarser layer formed by crystals of β-spodumene$_{ss}$ and zircon could create residual stress in order to exhibit increased apparent fracture toughness and energy absorption.

4. Conclusions

Taking into account some interesting thermal and dielectric properties, a selected β-spodumene-based glass ceramic composition ($16.9Li_2O \cdot 5.0ZrO_2 \cdot 65.1SiO_2 \cdot 8.6Al_2O_3$) was used for crystallization kinetics investigation by means of Nonisothermal method. The crystallization mechanism was found to be predominantly surface crystallization when the particle size is small. Two crystallization fronts regarding the crystalline phases formed, β-spodumene$_{ss}$ and zircon, were identified starting at approximately 670°C and 700°C, respectively. The morphology of the microstructures showed a columnar structure for the former and a globular for the second one. Apparent activation energy for crystallization E_c was found to be in the range 274 kJ/mol with an Avrami parameter n of 1 that is compared very favorably with SEM observations. At 850°C/10 min, a low-porosity (3.2%), low-CTE ($2.38 \times 10^{-6\circ}C^{-1}$), low-dielectric constant (9.97 ± 0.84) material was obtained. Moreover, the dielectric loss at 1 MHz was <0.3%. A value of 386 kJ·mol^{-1} was obtained for the activation energy of structural relaxation E_{relax}, in which its value is significantly higher than the activation energy for crystallization, hindering densification of material.

Acknowledgments

The authors are grateful to the Brazilian Foundation for the Coordination of Higher Education Graduate Training (CAPES), to the National Council of Scientific and Technological Development (CNPq), and to the German Foundation for Interchange (DAAD) for supporting this work.

References

[1] R. R. Tummala, "Ceramic and glass ceramic packaging in the 1990s," *Journal of the American Ceramic Society*, vol. 74, pp. 895–908, 1991.

[2] Y. Shimada, K. Utsumi, M. Suzuki, H. Takamizawa, M. Nitta, and T. Watari, "Low firing temperature multilayer glass ceramic substrate," *IEEE Transactions on Components, Hybrids, and Manufacturing Technology*, vol. 6, no. 4, pp. 382–388, 1983.

[3] C. R. Chang and J. H. Jean, "Crystallization kinetics and mechanism of low-dielectric, low-temperature, cofirable CaO-B_2O_3-SiO_2 glass-ceramics," *Journal of the American Ceramic Society*, vol. 82, no. 7, pp. 1725–1732, 1999.

[4] O. R. K. Montedo, F. M. Bertan, R. Piccoli, D. Hotza, A. N. Klein, and A. P. N. de Oliveira, "Low thermal expansion sinterered LZSA glass-ceramics," *American Ceramic Society Bulletin*, vol. 87, no. 7, pp. 34–40, 2008.

[5] C. M. Gomes, A. P. N. Oliveira, D. Hotza, N. Travitzky, and P. Greil, "LZSA glass-ceramic laminates: fabrication and mechanical properties," *Journal of Materials Processing Technology*, vol. 206, no. 1–3, pp. 194–201, 2008.

[6] O. R. K. Montedo, F. J. Floriano, J. de Oliveira Filho, E. Angoletto, and A. M. Bernardin, "Sintering behavior of LZSA glass-ceramics," *Materials Research*, vol. 12, no. 2, pp. 197–200, 2009.

[7] C. M. Gomes, C. R. Rambo, A. P. N. de Oliveira et al., "Colloidal processing of glass-ceramics for laminated object manufacturing," *Journal of the American Ceramic Society*, vol. 92, no. 6, pp. 1186–1191, 2009.

[8] W. A. Johnson and R. F. Mehl, "Reaction kinetics in processes of nucleation and growth," *AIME Transactions*, vol. 135, pp. 416–442, 1939.

[9] I. W. Donald and B. L. Metcalfe, "Thermal properties and crystallization kinetics of a sodium aluminophosphate based glass," *Journal of Non-Crystalline Solids*, vol. 348, pp. 118–122, 2004.

[10] A. Marotta, A. Buri, and F. Branda, "Surface and bulk crystallization in non-isothermal devitrification of glasses," *Thermochimica Acta*, vol. 40, pp. 397–403, 1980.

[11] F. Branda, "Nucleation and crystal growth in inorganic glass-forming systems: a DTA study," *Thermochimica Acta*, vol. 203, pp. 373–378, 1992.

[12] I. W. Donald, "The crystallization kinetics of a glass based on the cordierite composition studied by DTA and DSC," *Journal of Materials Science*, vol. 30, no. 4, pp. 904–915, 1995.

[13] A. P. N. de Oliveira, A. B. Corradi, L. Barbieri, C. Leonelli, and T. Manfredini, "The effect of the addition of $ZrSiO_4$ on the crystallization of $30Li_2O/70SiO_2$ powdered glass," *Thermochimica Acta*, vol. 286, no. 2, pp. 375–386, 1996.

[14] Y. Hu and C. L. Huang, "Crystallization kinetics of the $LiNbO_3$-SiO_2-Al_2O_3 glass," *Journal of Non-Crystalline Solids*, vol. 278, no. 1–3, pp. 170–177, 2000.

[15] H. Shao, K. Liang, and F. Peng, "Crystallization kinetics of MgO-Al_2O_3-SiO_2 glass-ceramics," *Ceramics International*, vol. 30, no. 6, pp. 927–930, 2004.

[16] E. R. Shaaban, "Non-isothermal crystallization kinetic studies on a ternary, $Sb_{0.14}As_{0.38}Se_{0.48}$ chalcogenide semi-conducting glass," *Physica B*, vol. 373, no. 2, pp. 211–216, 2006.

[17] M. S. Bapna and H. J. Mueller, "Thermodilatometric characterization for devitrification of a micaceous dental glass-ceramic," *Journal of the American Ceramic Society*, vol. 82, no. 7, pp. 1771–1776, 1999.

[18] B. Karmakar, P. Kundu, S. Jana, and R. N. Dwivedi, "Crystallization kinetics and mechanism of low-expansion lithium aluminosilicate glass-ceramics by dilatometry," *Journal of the American Ceramic Society*, vol. 85, no. 10, pp. 2572–2574, 2002.

[19] R. K. Thakur and S. Thiagarajan, "Studies in catalyzed crystallization of glasses: a DTA method," *Glass and Ceramic Bulletin*, vol. 13, pp. 33–45, 1966.

[20] C. T. Moynihan, A. J. Easteal, M. A. Debolt, and J. Tucker, "Dependence of the fictive temperature of glass on cooling rate," *Journal of the American Ceramic Society*, vol. 59, pp. 12–16, 1976.

[21] H. E. Kissinger, "Variation of peak temperature with heating rate in differential thermal analysis," *Journal of Research of the National Bureau of Standards*, vol. 57, pp. 217–221, 1956.

[22] T. Ozawa, "Kinetics of non-isothermal crystallization," *Polymer*, vol. 12, no. 3, pp. 150–158, 1971.

[23] J. A. Augis and J. E. Bennett, "Calculation of the Avrami parameters for heterogeneous solid state reactions using a modification of the Kissinger method," *Journal of Thermal Analysis*, vol. 13, no. 2, pp. 283–292, 1978.

[24] K. Lee, D. A. Hirschfeld, and J. J. Brown, "In situ whisker-reinforced β-eucryptite glass-ceramic: I, morphology and crystallization kinetics," *Journal of the American Ceramic Society*, vol. 79, no. 3, pp. 597–602, 1996.

[25] A. M. Hu, M. Li, D. L. M. Dali, and K. M. Liang, "Crystallization and properties of a spodumene-willemite glass ceramic," *Thermochimica Acta*, vol. 437, no. 1-2, pp. 110–113, 2005.

[26] E. M. Rabinovich, "Preparation of glass by sintering," *Journal of Materials Science*, vol. 20, no. 12, pp. 4259–4297, 1985.